BNL-NUREG-39412

THERMAL-HYDRAULIC STUDIES ON MOLTEN CORE-CONCRETE INTERACTIONS*

G. A. Greene
Brookhaven National Laboratory
Department of Nuclear Energy
Upton, New York 11973

BNL-NUREG--39412

TI87 006905

Recent assessments of risk due to unterminated severe accidents in light water power reactors have indicated that the consequences of molten core-concrete interactions (MCCI) dominate the considerations of containment loads and performance, as well as the release of non-volatile fission product aerosols to the containment building [1,2]. The issues of containment pressurization, combustible gas generation, structural erosion, fission product release, and fission product decontamination are critical in the evaluation of risk as currently being quantified by the Severe Accident Risk Reevaluation Program (SARRP) [3]. The program at BNL has focused on investigating several important aspects of MCCIs in an effort to support the integral melt-concrete programs as well as the CORCON [4] and VANESA [5] computer code development and verification programs at SNL. Experimental, analytical, and computational programs are currently underway to investigate and support validation of a variety of physical processes that occur during a MCCI, including interlayer heat and mass transfer, liquid-liquid boiling processes, and aerosol formation and decontamination [6,7].

Interlayer heat and mass transfer refers to processes that occur within a core melt between the stratified, immiscible phases of core oxides and metals. Associated with this category of phenomena are pool boil-up and void fraction, distribution of phases and heat sources, onset and rate of mass entrainment, and the rate of interlayer heat transfer. Liquid-liquid boiling processes refer to those processes that may occur at either the melt-concrete or melt-coolant interface. Associated with this category of phenomena are the rate of coolant boiling, gas film stability and melt-concrete heat transfer, enhancement of film boiling by non-condensable gas injection, and the general phenomenon of stratified layer steam explosions. Aerosol formation and decontamination refer to the processes that occur at a melt-atmosphere or a melt-coolant interface under the condition of gas bubbling from below, creating aerosols by mechanical processes or decontaminating aerosols from the gas stream, respectively. The first two of these three areas of current research will be discussed in greater detail in the sections to follow.

1. Interlayer Heat and Mass Transfer

The issue of interlayer heat and mass transfer addresses the phenomena that occur primarily interior to the molten core debris itself. At issue here are the boil-up and void distribution, two-phase flow regime, layer temperatures, distribution of phases, heat sources and fission products, and the rate of interlayer heat transfer and mass entrainment.

*Work performed under the auspices of the U.S. Nuclear Regulatory Commission.

Void distribution has been investigated experimentally in bubbling pools with gas injection from below to simulate concrete decomposition gas blowing into molten corium [7]. Adiabatic tests with air injection into water were performed as well as two-fluid interfacial heat transfer tests. These results are shown in Figure 1, compared to the drift flux void fraction model in the CORCON code. The data demonstrate good agreement with the drift flux model, approaching a maximum limit of approximately 0.40 at a superficial gas velocity of 60 cm/s. The data indicate that the dominant flow regimes are bubbly and churn turbulent. For other phenomena of interest, it is suggested that the experimental gas injection superficial velocity attempt to cover this range in order to span the appropriate flow regimes.

Subsequent efforts in this investigation were directed to the characterization of the rate of heat transfer between overlying immiscible liquid layers agitated by gas bubbling from below. The results of the earliest such tests are presented in Figure 2 in terms of the interlayer heat transfer coefficient vs the superficial gas injection velocity [8,9,10]. It was immediately apparent from the experimental data and visual observations of the test apparatus that two regimes of heat transfer behavior may exist: stratified interlayer heat transfer, and entrainment heat transfer. Specifically, the experiments with liquid metal and oil (or water) demonstrated a well-defined interface between the liquid layers and a low rate of interlayer heat transfer, while the oil-water experiments were visually observed to undergo intense mass entrainment and a rate of interlayer heat transfer that was as much as an order of magnitude greater than the separated case. Since the stratified, gas-sparged geometry was the condition assumed in the structure of CORCON modeling, this was the first system studied in depth.

An example of the gas-sparged enhanced liquid-liquid heat transfer without entrainment is shown in Figure 3 [11]. There the data for oil-liquid metal and water-liquid metal are shown compared to the original Szekely surface renewal heat transfer model [12]. Although better agreement with the data is achieved than with the original Konsetov model in CORCON-MOD1, the model shown is clearly inadequate, underpredicting both the magnitude and the trend of the data. To resolve this apparent difficulty, additional heat transfer experiments were performed with fluid pairs of both mercury-silicone oil and mercury-water. The resulting data base was correlated in dimensionless form over two orders of magnitude in Prandtl number and nearly three orders of magnitude in bubble Reynolds number. The results of this dimensionless correlation are shown in Figure 4. The correlation shown in the figure is that currently used in CORCON-MOD2 for liquid-liquid interlayer heat transfer with gas-sparging from below [13].

Recognizing that bubble-induced mass entrainment had earlier been shown to dominate interlayer heat transfer for certain liquid pairs, attention was shifted to resolve the issues of bubble-induced entrainment onset, mass entrainment rate, and entrainment heat transfer. The ability to predict the onset of bubbling-induced mass transfer between overlying immiscible liquid layers is necessary in order to make a determination of whether stratification or mixing will occur for both phase distribution and heat transfer.

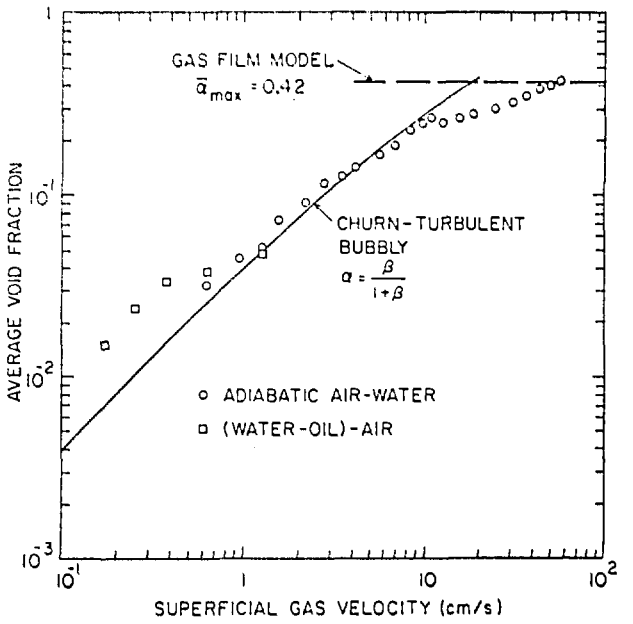

Figure 1 Void Fraction in Liquid Pools with Gas Injection from Below

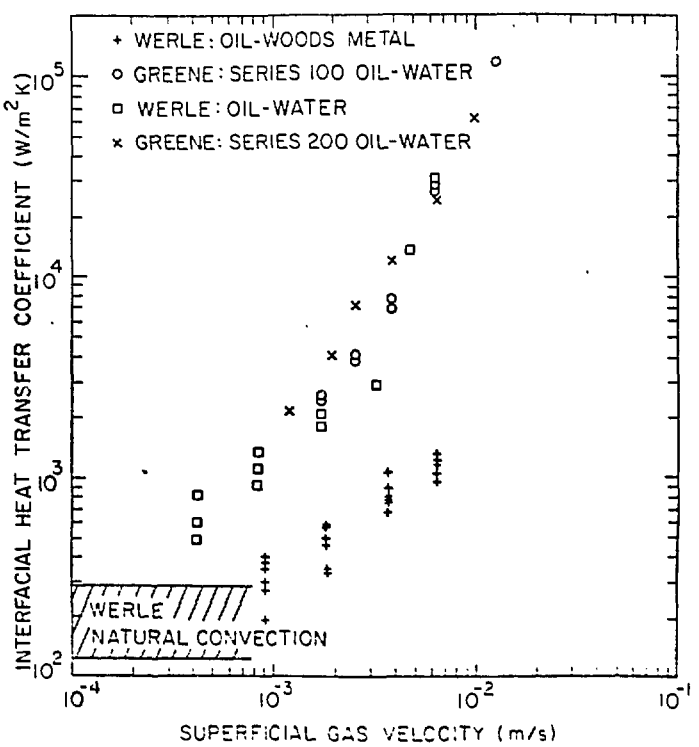

Figure 2 Comparison of Entrainment and Non-Entrainment Heat Transfer Between Immiscible Liquids with Bottom Gas Sparging

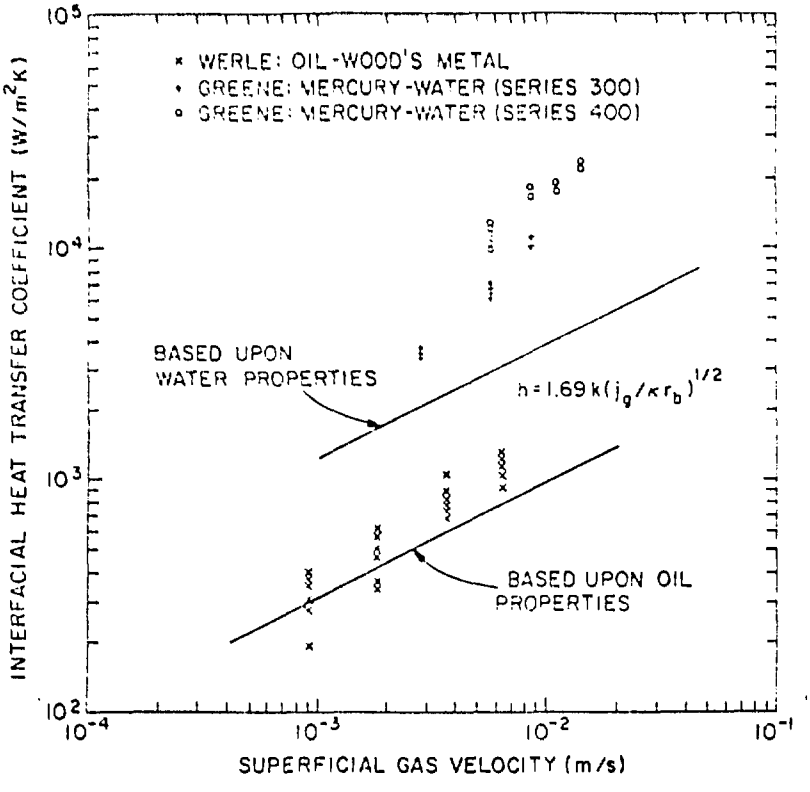

Figure 3 Gas-Sparged Enhanced Liquid-Liquid Heat Transfer Without Entrainment

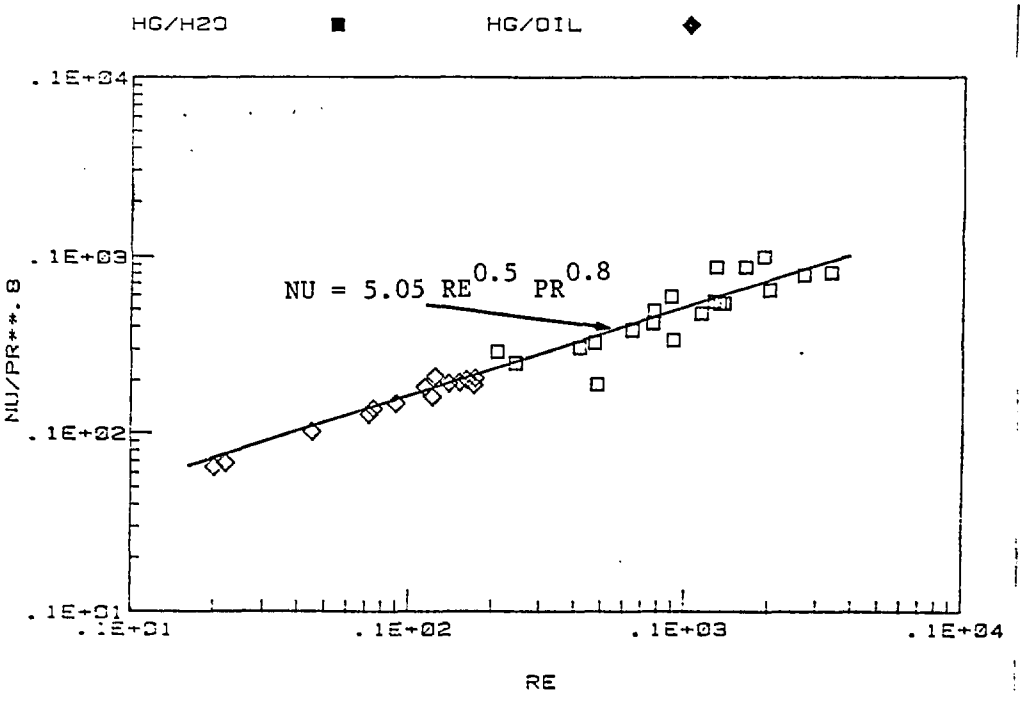

Figure 4 Dimensionless Correlation of Interlayer Heat Transfer Data Without Entrainment

Experiments were initiated to investigate the necessary and sufficient conditions to promote bubble-induced entrainment across a stratified liquid-liquid interface. Several pairs of immiscible liquids were tested. These included 10 cs. silicone oil-water, 100 cs. silicone oil-water, water-R11, acetone-glycerine, hexane-water, and bromoform-water. In addition, an observed data point for bismuth-bismuth slag was included. The data for some of these liquid pairs is shown in Figure 5. Open symbols indicate cases with no observed entrainment; solid symbols indicate cases in which entrainment was measured. The comparison of these data to the entrainment onset model which was developed (solid line) is at this point preliminary. Final data analysis will be performed when more precise measurements of the fluid physical and transport properties are complete, in particular the liquid-liquid interfacial tension. Nevertheless, very good agreement is shown between the entrainment onset model and the data. Also shown on Figure 5 are the predictions of the entrainment onset model for molten corium layers. It is shown that depending on the physical properties of the melt, corium layers are predicted to stratify or entrain depending upon the assumed bubble diameter. In fact, an increase in bubble diameter from 0.75 cm to 1.0 cm is calculated to be sufficient to drive the melt from stratified to a mixed condition. Therefore, it is clearly necessary to be able to calculate heat and mass transfer due to bubble-induced entrainment as well as stratified layer heat transfer.

Subsequently, experiments were performed to investigate the rate of mass entrainment between overlying immiscible liquid layers due to rising bubbles. The procedure employed was identical to that used to determine entrainment onset; however for the entrainment rate tests, the volume of entrained fluid was physically intercepted and measured. The results from four series of tests are shown in Figure 6. Without going into details, the fluid pairs shown were chosen to test the effects of density ratio, liquid-liquid interfacial tension, and fluid viscosity. For the fluid pairs with a density ratio closest to unity, namely the oil-water fluid pairs, the measured entrained volume was the greatest. Note the viscosity of the upper fluid did not have any impact on the entrainment. For the two other fluid pairs, the density ratio was 0.63. Increasing the difference in density between the fluid layers had the effect of reducing the entrainment. The significant reduction in entrainment experienced by the acetone-glycerine pair, however, was due to the extremely high value of the lower fluid viscosity; this had the effect of reducing the momentum of the rising bubble and further reducing the entrainment. All these effects are incorporated in the analytical model for bubbling-induced entrainment which is currently under development and expected to be completed in the near future. It is apparent that calculation of the entrainment rate depends upon accurate and reliable knowledge of the bubble dynamics as well as the physical and transport properties of the melt.

Once the hydrodynamics of interlayer entrainment have been characterized, it is a relatively simple matter to calculate the interlayer heat transfer. A model has been reported which describes the entrainment heat transfer process as a superposition of the interlayer heat transfer rate augmented by a contribution due to the mass entrainment [8]. It is assumed that under most circumstances, all or nearly all of the excess enthalpy of the entrained fluid is transferred to the continuous phase prior to settling out. This process is, in practice, calculated as a function of the Biot number and Fourier number of the entrained mass to determine precisely what fraction of the excess enthalpy

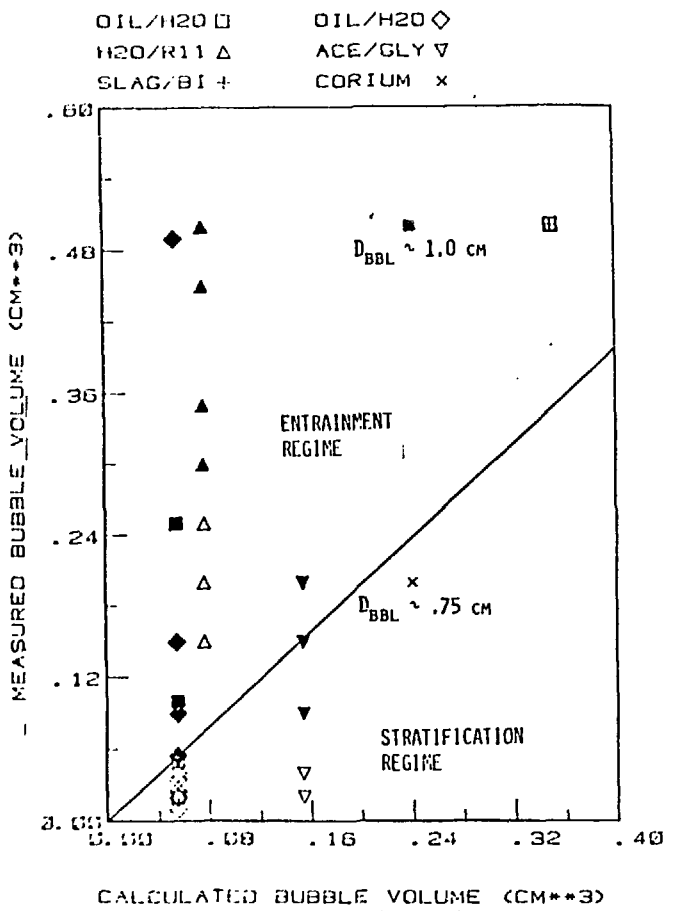

Figure 5 Comparison of Entrainment Onset Model to Single Bubble Data

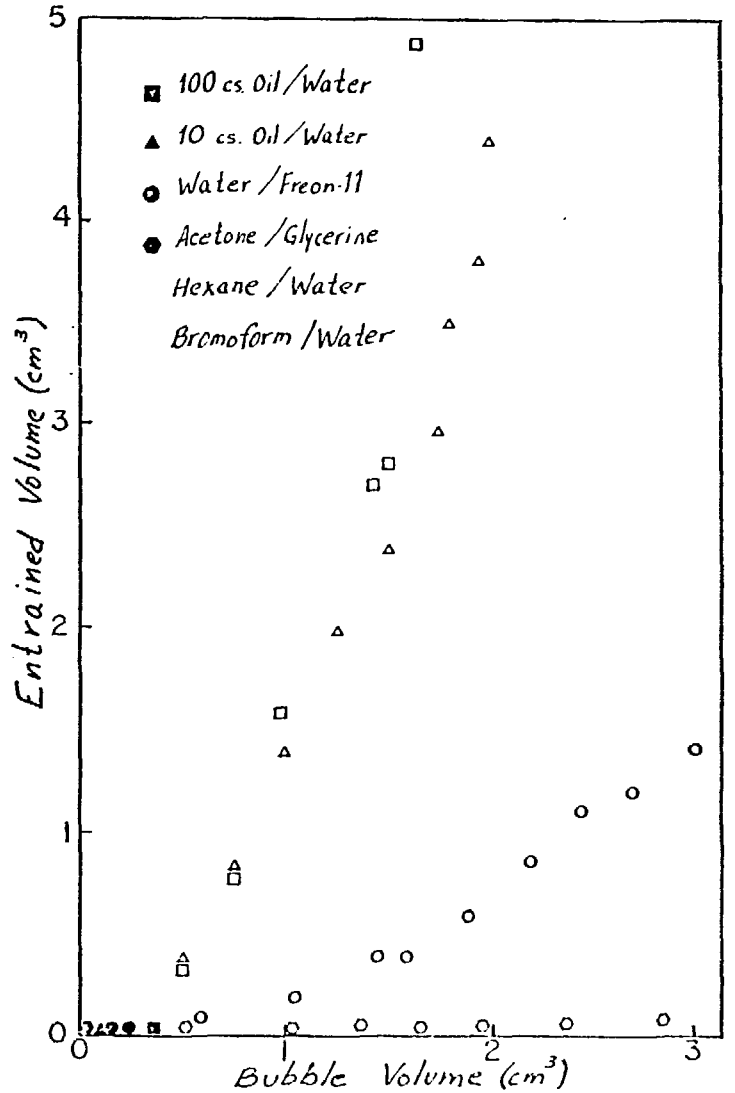

Figure 6 Single Bubble Entrainment Data vs. Bubble Volume

is actually lost. In other words, a rigorous analysis is performed to determine the approach to equilibrium between the entrained fluid and the continuous fluid. Clearly, the last piece of information needed to completely model the interlayer processes between overlying immiscible liquid layers with bubble agitation is a model to describe the rate of settling of the entrained phase back into its original layer. The physical state of the melt will depend upon the rate of settling compared to the rate of entrainment. If the settling rate can be balanced by the entrainment rate, an equilibrium mixture layer can be maintained. If, however, settling cannot keep pace with entrainment, the end result will be melt homogenization.

A complete package of mechanistic models to describe the interlayer heat and mass transfer processes is nearing completion; upon completion, this package will be incorporated into the CORCON-MOD2 computer code in order to assess the impact of interlayer heat and mass transfer process upon the ex-vessel source term calculations.

2. Liquid-liquid Boiling Processes

The issues of liquid-liquid film boiling and pseudo-film boiling address the phenomena that occur primarily on the periphery of the molten core debris, either at the melt-concrete interfaces or at the melt-coolant interface. At issue here are the pool thermal behavior, mode and rate of pool solidification, rate of boiling of reactor coolant over molten or partially solidified core debris, effect of non-condensable gas flux on liquid-liquid film boiling, and the frequency, efficiency, and resulting debris size distribution due to steam explosions from the layered geometry characteristic of MCCI's [14].

Among the earliest experiments performed with respect to liquid-liquid boiling processes were investigations into the thermal behavior of bubbling melts subjected to boiling from above. The questions to be answered here were "how do melt pools cool, both temporally and spatially," and "what is the mode of solidification of bubbling pools with overlying pools of coolant?" Some of the results for a characteristic experiment are shown in Figure 7. In these two graphs we see the superposition of seven micro-thermocouples in a lead melt subject to gas injection from below and boiling of saturated R11 above. Note that the pool is isothermal, cooling with no spatial temperature gradient. The rate of cooling in this instance was precisely determined by the film boiling heat flux boundary condition imposed at the upper surface. When the melt pool cooled to its solidification temperature, it was observed to remain at that temperature for a considerable period of time with no evidence of crusting. During this period, the mode of solidification of the pool was by formation of a slurry. This persisted in the experiment for approximately 70 seconds, after which time stable crusting was able to be supported by the bubbling melt. The evidence supplied by this data suggest that the assumption implicit in the CORCON development of crusting may need to be reexamined in order to allow for the three regions identified in this data: molten pool with no freezing, freezing as a slurry due to crust instability,and stable crusting.

Attention was directed toward investigating the mode and magnitude of the boiling heat flux of saturated reactor coolant over molten core-concrete interactions. Due in part to the activities of the CLWG [2] as well as an

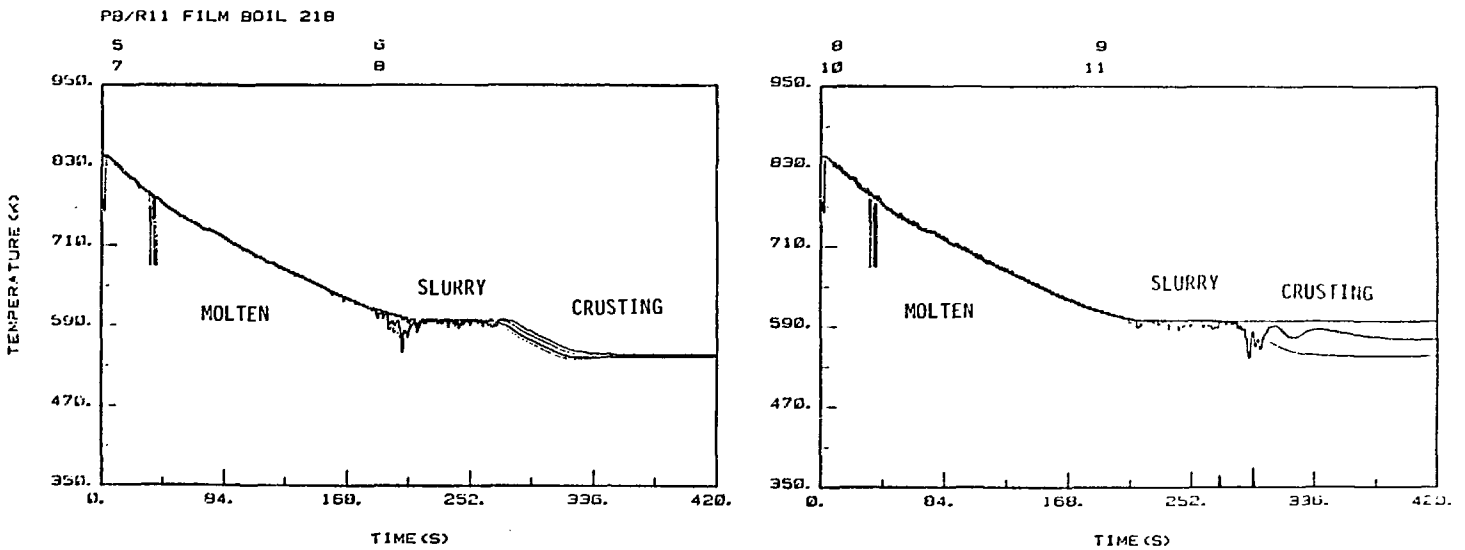

Figure 7 Transient Thermal Behavior of Molten Bubbling Pools with Coolant Boiling Above

assessment of the state-of-the-art of MCCI modeling for source term application [5], provisions for coolant layer boiling were included in the CORCON-MOD2 code. Boiling of water over a MCCI would be complicated by the presence of a molten heat transfer surface as well as non-condensable gas blowing from below. However, there was no data base with which to evaluate either of these two effects. Assuming that the MCCI would be hot enough that the coolant layer would be in the film boiling regime, it was decided to implement the Berenson flat plate film boiling model [15] into CORCON-MOD2 [4].

Experiments were initiated to examine the magnitude of the film boiling heat flux for various saturated coolants over molten pools of liquid metal. In this fashion, the effect of the molten heating surface could be examined, neglecting for the moment the effect of the non-condensable concrete decomposition gases. A sample of the experimental results for saturated water in film boiling over molten pools of lead, bismuth, and Wood's metal is shown in Figure 8. For the most part, the data show good agreement with the Berenson flat plate film boiling model when there is no non-condensable gas injection. The data for R11 and liquid metal melts exhibited similar good agreement with Berenson. More details of these tests may be found in References 16-18.

Subsequently, several series of experiments were performed with R11 and water over bubbling liquid metal melts to examine the effect of a non-condensable gas flux from below upon liquid-liquid film boiling. The gas injection was to simulate the effect of concrete decomposition gases bubbling through the melt and across the film boiling interface. An example of the resulting data shown in Figure 9 for the case of saturated water over liquid metal melts. It was found that the boiling heat flux was a monotonically increasing function of the gas injection superficial velocity. A very much similar behavior was found for saturated R11 in film boiling over bubbling liquid metal pools as well [19]. For the case of gas flux-enhanced film boiling of water, the data were shown to exceed the Berenson flat plate film boiling limit by as much as a factor of six at a superficial gas velocity of less than 3 cm/s. This effect is clearly neglected in the present coolant layer modeling in CORCON-MOD2. It is recommended that a simple correlational approach be adopted in order to quickly assess the impact of this gas flux-enhanced film boiling phenomenon upon such issues as steam production, melt temperature, containment pressurization, and hydrogen burning.

The liquid-liquid film boiling tests with water were always unstable and chaotic as opposed to the tests done with R11 over the same melts, which were by contrast quiescent. Visual observations made of the liquid-liquid boiling interface between both R11 and water with liquid metal melts revealed a startling difference in behavior. While the R11 liquid metal liquid-liquid film boiling interface was smooth and undisturbed with nearly a mirror-like finish, the water-liquid metal interface was irregular and agitated with evidence of liquid-liquid contact and spiking of melt upwards into the water pool [14]. In the heat transfer experiments performed with water and liquid metal melts, this unstable behavior nearly always resulted in an explosive boiling interaction or steam explosion. These steam explosions from the stratified geometry were self-destabilizing, and could be multiple as long as water and melt were available in the test vessel. An example of this behavior is shown in Figure 10 for Run 419. In these tests, a liquid-filled pressure probe was immersed

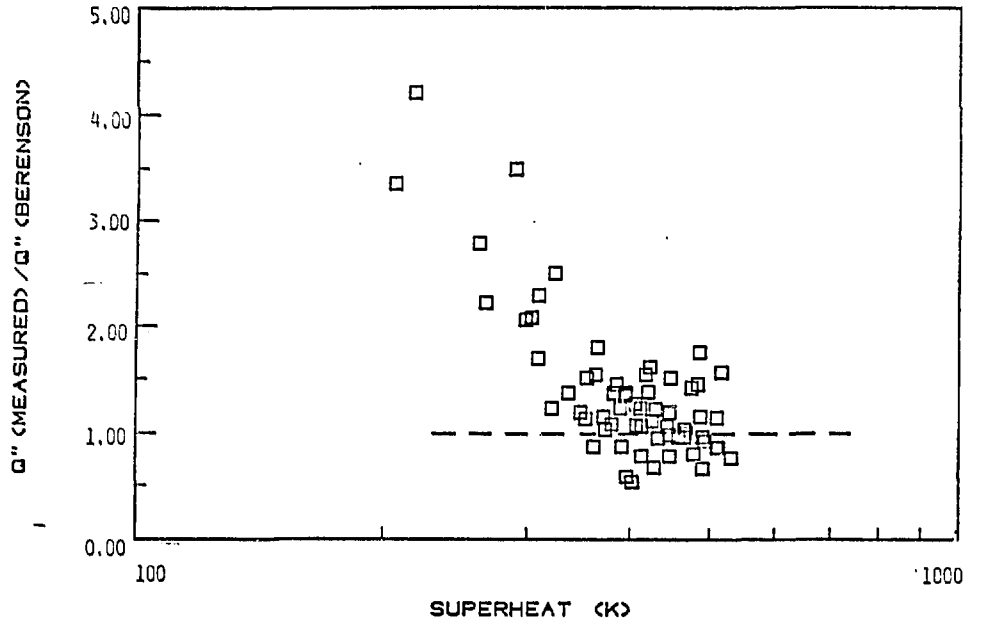

Figure 8 Liquid-Liquid Film Boiling of Saturated Water Over Molten Metal Pools with Zero Gas Injection

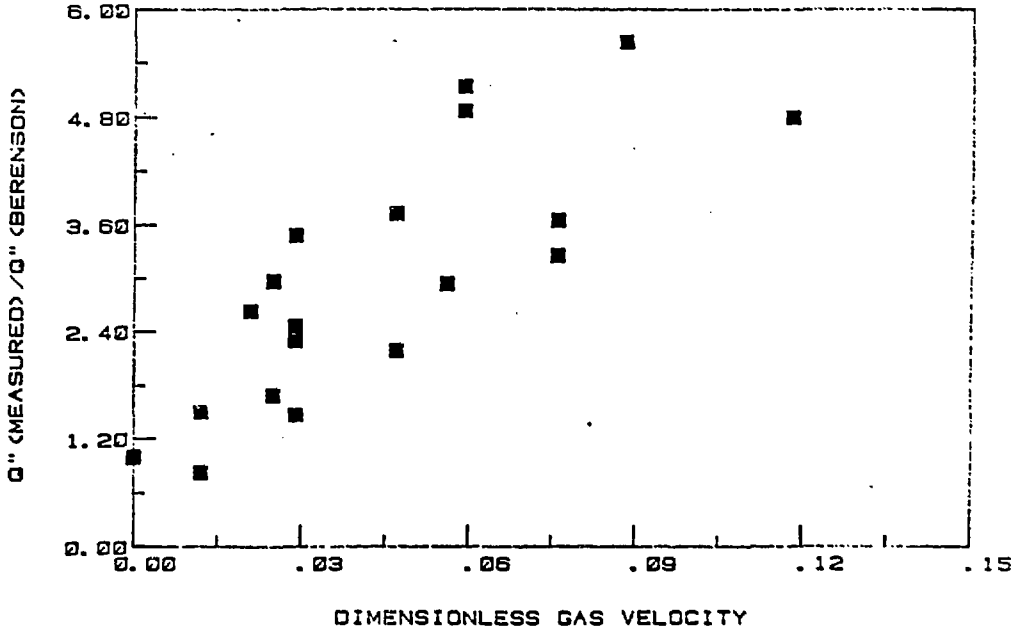

Figure 9 Effect of Non-Condensable Gas Injection on Film Boiling of Saturated Water Over Molten Metal Pools

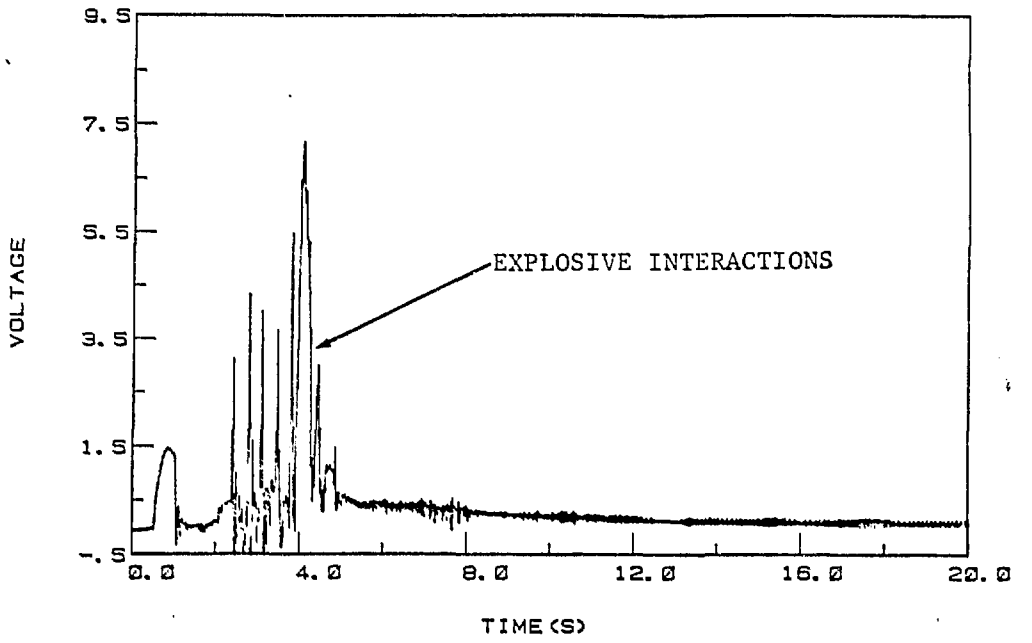

Figure 10 Pressure Spikes Due to Multiple Steam Explosions in Run 419 (Water Boiling over Liquid Metal, Superficial Gas Injection = 0.90 cm/s)

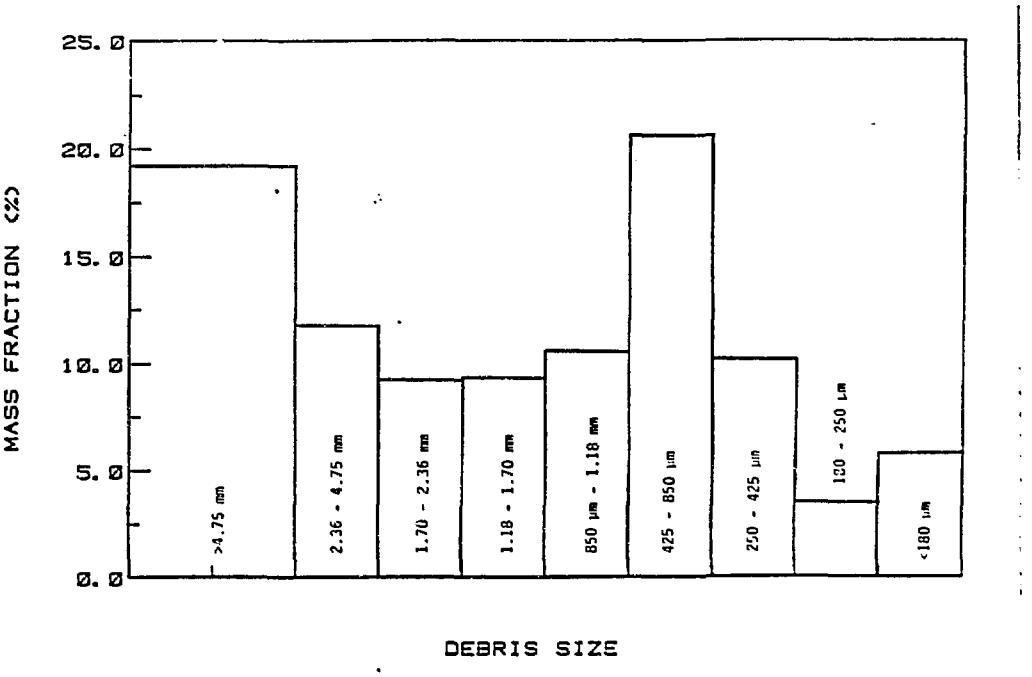

Figure 11 Debris Size Distribution Resulting from Explosive Interaction During Liquid-Liquid Film Boiling (Run 418)

in the boiling coolant layer in order to record any pressurization events. These events are supported by simultaneous temperature measurements and a video tape of the test. The pressure probe was of low frequency response and is useful as an event marker. At approximately two seconds after initiation of the test, a series of eight steam explosions occurred in rapid succession. The last occurred at five seconds. The explosive interactions increased in intensity until the sixth event; starved for water, the succeeding two events were mild in comparison. These events essentially interrupted the liquid-liquid film boiling stage of the test which was again resumed after the last explosive interaction. In Run 419, there was a non-condensable superficial gas injection from below of approximately 0.90 cm/s.

The explosive interactions cause a rapid transfer of heat from the melt to the water, generally resulting in the generation of solidified debris which is thrown from the interaction vessel and collects in the test enclosure. This debris was carefully collected and sieved in order to determine the size distribution of the solid particles resulting from these tests. An example of such a debris size distribution, in this case resulting from Run 418, is shown in Figure 11 [20]. The size distribution shown in Figure 11 is characteristic of the debris from all the tests performed to date. The distribution is apparently tri-modal, exhibiting peaks in the following size ranges: (a) greater than 4.75 mm, (b) 425-850 μm, and (c) less than 180 μm. The peak in the range 425-850 μm is not unlike the mass mean particle size in the SNL high pressure melt ejection studies currently underway. If a mixing efficiency of such a test is defined as the debris mass less than 425 μm divided by the total debris generated, such mixing efficiencies are calculated to be in the range 10-20%. Explosive efficiency has yet to be measured.

Current understanding of coolant layer dynamics suggests that coolant boiling will involve periods of gas flux-enhanced film boiling, interrupted by periods of destabilization and explosive interactions. It is presently planned to evaluate these phenomena parametrically within the existing structure of CORCON-MOD2, to determine the impact of such modeling upon steam generation and containment loading, melt temperature, debris bed generation, and structural loading.

REFERENCES

1. Silberberg, M., et al., "Reassessment of the Technical Bases for Estimating Source Terms," NUREG-0956 (July 1986).

2. Containment Loads Working Group, "Estimates of Early Containment Loads from Core Melt Accidents," NUREG-1079 (December 1985).

3. NUREG-7750 (in preparation).

4. Cole, R.K., D.P. Kelly, and M.A. Ellis, "CORCON-MOD2: A Computer Program for Analysis of Molten Core-Concrete Interactions," NUREG/CR-3920 (August 1984).

5. Powers, D.A., J.E. Brockmann, and A.W. Schiver, "VANESA: A Mechanistic Model of Radionuclide Release and Aerosol Generation During Core Debris Interactions with Concrete," NUREG/CR-4308 (July 1986).

6. Greene, G.A., et al., "Quarterly Progress Reports for Safety Research Programs Sponsored by Office of Nuclear Regulatory Research, NUREG/CR-2331.

7. Greene, G.A., and D.A. Powers, in "Review of the Status of Validation of the Computer Codes used in the Severe Accident Source Term Reassessment Study (BMI-2104)," edited by T.S. Kress, ORNL/TM-8842 (April 1985).

8. Greene, G.A., and C.E. Schwarz, "An Approximate Model for Calculating Overall Heat Transfer Between Overlying Immiscible Liquid Layers with Bubble-Induced Liquid Entrainment," Post Accident Debris Cooling Meeting, Karlsruhe, FRG (July 1982).

9. Greene, G.A., and C.E. Schwarz, "Interfacial Heat Transfer Between Overlying Liquid Layers with Gas Agitation," Trans. Am. Nucl. Soc., 39, (November 1981).

10. Werle, H., "Enhancement of Heat Transfer Between Two Horizontal Liquid Layers by Gas Injection at the Bottom," Nuclear Technology, 59, (October 1982).

11. Greene, G.A., et al., "Heat Transfer Between Immiscible Liquids Enhanced by Gas Bubbling," International Meeting on Thermal Nuclear Reactor Safety, Chicago, IL (September 1982).

12. Szekely, J., "Mathematical Model for Heat or Mass Transfer at the Bubble-Stirred Interface of Two Immiscible Liquids," Int. J. Heat Mass Transfer, 6, pp 417-422 (1963).

13. Greene, G.A., and T.F. Irvine, "Heat Transfer Between Overlying Immiscible Liquid Layers Driven by Gas Bubbling Across the Interface," 24th ASME-AIChE National Heat Transfer Conference, Pittsburg, PA (August 1987).

14. Greene, G.A., et al., "Some Observations on Simulated Molten Debris-Coolant Layer Dynamics," International Meeting on Light Water Reactor Severe Accident Evaluation, Cambridge, MA (August 1983).

15. Berenson, P.J., "Film Boiling Heat Transfer from a Horizontal Surface," J. Heat Transfer, 83, pp. 351-358 (1961).

16. Greene, G.A., et al., "Liquid-liquid Film Boiling of R-11 on Liquid Metal," Trans. Am. Nucl. Soc., 45, p. 466 (November 1983).

17. Greene, G.A., and T.F. Irvine, "Film Boiling of R-11 on Liquid Metal Surfaces," Eighth International Heat Transfer Conference, 4, pp 2049-2054, San Francisco, CA (August 1986).

18. Greene, G.A., C. Finfrock, and S.B. Burson, "The Effects of Water in Film Boiling Over Liquid Metal Melts," Trans. Am. Nucl. Soc., 53, pp. 360-362 (November 1986).

19. Greene, G.A., "Gas-Bubbling Enhanced Film Boiling of Freon-11 on Liquid Metal Pools," Trans. Am. Nucl Soc., 49, pp. 249-251 (June 1985).

20. Greene, G.A., "Separate Effects Studies Related to Core-Concrete Interactions and Aerosol Behavior," USNRC/BMFT Core Meltdown Information Meeting, Cologne, FRG (October 1986).

DISCLAIMER